32. I. A. Wilson, J. M. Rini, D. H. Fremont, G. G. Fieser, E. A. Stura, *Methods Enzymol.* **203**, 153 (1991).
33. D. Rognan, M. J. Reddehase, U. H. Koszinowski, G. Folkers, *Proteins Struct. Funct. Genet.* **13**, 70 (1992).
34. J. H. Brown *et al.*, *Nature* **332**, 845 (1988).
35. M. M. Davis and P. J. Bjorkman, *ibid.* **334**, 395 (1988).
36. C. Chothia, D. R. Boswell, A. M. Lesk, *EMBO J.* **7**, 3745 (1988).
37. D. R. Davies, E. A. Padlan, S. Sheriff, *Annu. Rev. Biochem.* **B59**, 439 (1990).
38. K. Shibata, M. Imarai, G. M. van Bleek, S. Joyce, S. G. Nathenson, *Proc. Natl. Acad. Sci. U.S.A.* **89**, 3135 (1992).
39. T. S. Jardetzky *et al.*, *EMBO J.* **9**, 1797 (1990); J. L. Maryanski, A. S. Verdini, P. C. Weber, R. R. Salemme, G. Corradin, *Cell* **60**, 63 (1990).
40. A. G. Amit, R. A. Mariuzza, S. E. V. Phillips, R. J. Poljak, *Science* **233**, 747 (1986).
41. J. A Bluestone, S. Jameson, S. Millár, R. Dick, in preparation; B. Catipovic, J. DalPorto, M. Mage, T. E. Johansen, J. P. Schneck, in preparation.
42. F. R. Carbone and M. J. Bevan, *J. Exp. Med.* **169**, 603 (1989).
43. A. J. Howard *et al.*, *J. Appl. Crystallogr.* **20**, 383 (1987).
44. P. D. M. Fitzgerald, *ibid.* **21**, 273 (1988).
45. The program HARADA (written by D. Filman and J. Arevalo) is based on a previously published algorithm [Y. Harada, A. Lifchitz, J. Berthou, *Acta Crystallogr.* **A37**, 398 (1981)].
46. A. T. Brünger, J. Kuriyan, M. Karplus, *Science* **235**, 458 (1987).
47. T. A. Jones, *J. Appl. Crystallogr.* 11, 268 (1978).
48. V. Luzatti, *Acta Crystallogr.* **5**, 802 (1952).
49. M. Carson, *J. Mol. Graphics* **5**, 103 (1987).
50. Tubes were generated with the program MCS TUBES (written by Y. Chen and A. Olson) and were rendered in the AVS environment [C. Upson *et al.*, *IEEE Comput. Graph. Appl.* **9**(no. 4), 30 (1989)].
51. To calculate solvent accessible surfaces we used a 1.4 Å radius probe and the program PQMS (written by M. L. Connolly), which is similar to the program MCS [M. L. Connolly, *J. Mol. Graph.* **3**, 19 (1985)].
52. We thank M. Pique for preparation of the figures, Y. Saito for production of the soluble H-2K^b, and J. Arevalo, N. Klinman, J. Bluestone, and R. Stanfield for helpful discussions. Supported in part by NIH grant CA-97489 (to P.A.P.) and training grant CA-09523 (to D.H.F.). This is publication 7467-MB from the Scripps Research Institute. Coordinates have been deposited in the Brookhaven Protein Data Bank and are available for prerelease.

24 June 1992; accepted 21 July 1992

Emerging Principles for the Recognition of Peptide Antigens by MHC Class I Molecules

Masazumi Matsumura, Daved H. Fremont,* Per A. Peterson, Ian A. Wilson

Class I major histocompatibility complex (MHC) molecules interact with self and foreign peptides of diverse amino acid sequences yet exhibit distinct allele-specific selectivity for peptide binding. The structures of the peptide-binding specificity pockets (subsites) in the groove of murine H-2K^b as well as human histocompatibility antigen class I molecules have been analyzed. Deep but highly conserved pockets at each end of the groove bind the amino and carboxyl termini of peptide through extensive hydrogen bonding and, hence, dictate the orientation of peptide binding. A deep polymorphic pocket in the middle of the groove provides the chemical and structural complementarity for one of the peptide's anchor residues, thereby playing a major role in allele-specific peptide binding. Although one or two shallow pockets in the groove may also interact with specific peptide side chains, their role in the selection of peptide is minor. Thus, usage of a limited number of both deep and shallow pockets in multiple combinations appears to allow the binding of a broad range of peptides. This binding occurs with high affinity, primarily because of extensive interactions with the peptide backbone and the conserved hydrogen bonding network at both termini of the peptide. Interactions between the anchor residue (or residues) and the corresponding allele-specific pocket provide sufficient extra binding affinity not only to enhance specificity but also to endure the presentation of the peptide at the cell surface for recognition by T cells.

The human and murine class I major histocompatibility complex (MHC) molecules are each separable into three allelic series of peptide-binding cell surface proteins, whose obligatory function is to present peptide antigens to cytotoxic T cells (*1–4*). Because of the extensive genetic polymorphism of these class I molecules, most individuals in an outbred population express two allelic forms of each isotype. Thus, the total number of class I molecules in an individual is very small compared with the entire repertoire of T cell receptors that can recognize a vast array of such peptides in the context of class I molecules.

Iso- and allotypic variants of class I molecules differ in those residues that form the peptide binding groove (*5, 6*). This observation suggests that individual class I molecules bind peptides with varying specificities. However, each class I molecule must be able to bind large sets of peptides to explain the broad discriminatory capacity of the immune system. Sequence analyses of peptides isolated from individual class I molecules have confirmed this notion (*7–10*). That is, endogenously bound peptides are restricted in length to eight or nine amino acids, and, despite the size limitation, almost any position in the peptide can accommodate many different amino acid residues. However, in certain positions, one or a few amino acid residues recur with considerably increased frequencies. Such residues, called "anchor" residues, are characteristic for each class I allotype examined, and presumably the side chains of these residues interact with allotype-specific residues in the peptide binding groove. However, in the absence of high-resolution crystallographic data on the class I molecule bound to defined peptide sequences, there has been little direct evidence to support this hypothesis.

Two structures of murine H-2K^b molecules complexed with different viral peptides have now been elucidated at 2.3 and 2.5 Å resolution (*11*). This information, in conjunction with the available information on the structures of three human histocompatibility antigen (HLA) class I molecules (*6, 12–14*) and the allele-specific peptide motifs (*9*), has permitted us to examine how class I molecules recognize and present a variety of chemically distinct peptides. We now show that conserved pockets at both ends of the peptide-binding groove accommodate the NH_2- and COOH-termini of peptides, whereas a deep polymorphic pocket in the middle of the groove forms the structural complementarity to the main anchor residue of the peptide and, hence, determines allele-specific peptide binding. Such limited usage of pockets appears to explain the broad but specific binding of peptides to MHC class I molecules.

Overall structure of peptide binding groove. We investigated the molecular mechanisms for MHC class I–peptide recognition by comparing structures of the murine class I molecule H-2K^b complexed with either VSV-8 peptide [vesicular stomatitis virus nucleoprotein(52–59); RGYVYQGL (*15*)] (*7*) or SEV-9 peptide [Sendai virus nucleoprotein(324–332); FAPGNYPAL) (*16*)] with the structure of the human class I molecule HLA-A2 (*5,*

M. Matsumura and P. A. Peterson are in the Department of Immunology and D. H. Fremont and I. A. Wilson are in the Department of Molecular Biology, The Scripps Research Institute, 10666 North Torrey Pines Road, La Jolla, CA 92037.

*D.H.F. is a graduate student in the Department of Chemistry, University of California–San Diego, La Jolla, CA 92093.

12, 13). The HLA-A2 structure was chosen for comparison because much is known about its peptide prefer-ences. For example, HLA-A2 selectively binds a nonapeptide with leucine at position 2 (Leu^{P2}) and valine at position 9 (Val^{P9}) (*9, 17, 18*), whereas H-2K^b preferentially binds an octapeptide with Tyr^{P5} or Phe^{P5} and Leu^{P8} (*9, 19*).

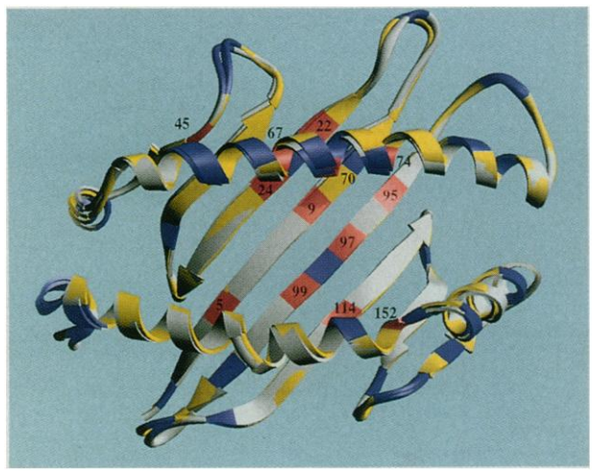

Fig. 1. Comparison of the $\alpha_1\alpha_2$ domains of H-2K^b molecule (yellow) superimposed onto the equivalent domains of HLA-A2 (white). All 52 polymorphic residues that differ in the $\alpha_1\alpha_2$ domain are shown on a ribbon trace (*42*) of the two class I molecules. The 13 residues that face into the groove are shown in red and numbered, whereas the others are shown in blue.

Table 1. The constituent residues of the peptide binding groove of H-2K^b. Surface areas were calculated from the refined coordinates of the H-2K^b–VSV-8 complex (excluding the coordinates of the peptide and water molecules) by employing the MS program (*40*). The listed residues have exposed surface areas when a 1.4 Å radius probe was used but buried when a 5.0 Å radius probe was used. Although residues Lys^{66} (pocket B), Ser^{73} (C/F), Thr^{80} (F), Tyr^{84} (F), Lys^{146} (F), Arg^{155} (D/E), Thr^{163} (A), and Trp^{167} (A) make van der Waals contacts with the peptides and hence constitute pockets (shown in parentheses), these residues are not included in the table since their side chains are exposed to the 5.0 Å probe. Residues Ala^{117} (pocket F) and Cys^{164} (A) are also omitted from the table since only the backbone atoms (O and Cα, respectively) are located within the groove.

Position	Residue	Pocket	Probe (Å)*	Location†
5	L (M)‡	A	3.0	
7	Y	A/B	3.5 (3.0)	
9	V (F)	B/C	3.0	
22	Y (F)	C (–)	3.0 (buried)	
24	E (A)	B	3.0	
34	V	– (B)	buried (3.0)	
45	Y (M)	B	3.0	
59	Y	A	3.5 (3.0)	
63	E	A/B	3.0	
67	A (V)	B	3.0	
70	N (H)	B/C	4.5 (>5.0)	Surface
74	F (H)	C	3.0	
77	D	F	4.5 (4.0)	Surface
81	L	F	3.0	
95	I (V)	F (–)	3.0 (buried)	
97	V (R)	C (C/E)	3.0 (4.5)	(Surface)
99	S (Y)	C/D (A/B/C/D)	3.5 (4.0)	(Surface)
114	Q (H)	C/D/E	4.0	Surface
116	Y	C/E/F (C/F)	3.0	
118	Y	F	3.5 (3.0)	
123	Y	F	3.0	
124	I	F (–)	3.0 (buried)	
143	T	F	3.0	
147	W	E/F	5.0	Surface
152	E (V)	E	4.5 (>5.0)	Surface
156	L	D/E	3.0 (5.0)	(Surface)
159	Y	A/D	4.0 (>5.0)	Surface
160	L	– (D)	buried (3.0)	
171	Y	A	3.0	

*The radius of probe to which residue becomes inaccessible. The term "buried" in this column indicates that residues are not accessible when 1.4 Å probe is used for the calculation. †Residues exposed to a >4.0 Å probe are categorized into "surface" residues; residues hidden from a <3.5 Å probe are considered "buried" residues. Pockets A, B, C, D, E, and F consist of 6 (7), 7 (9), 8 (7), 4 (5), 5 (5), and 9 (7) residues, respectively (the numbers in parentheses represent those of HLA-A2). Among them, "surface" residues are 1 (2), 1 (2), 2 (4), 2 (4), 3 (5), and 2 (2), leaving deep residues 5 (5), 6 (7), 6 (3), 2 (1), 2 (0), and 7 (5) for pockets A, B, C, D, E, and F, respectively. Thus, pockets A, B, C, and F are deep, and pockets D and E are shallow. ‡Residues, pockets, and probe radii corresponding to HLA-A2 are shown in parentheses. The coordinates of the HLA-A2 structure (*13*) were taken from the Brookhaven Protein Data Bank.

H-2K^b and HLA-A2 molecules differ at 108 positions. Of these, 52 residues differ in the $\alpha_1\alpha_2$ domains (~72 percent identity), 26 in the α_3 domain (~72 percent), and 30 in the β_2-microglobulin (~70 percent). Nevertheless, the overall structure of H-2K^b is remarkably similar to that of HLA-A2 (*11*, figure 1). In particular, the $\alpha_1\alpha_2$ domains of H-2K^b structures are almost indistinguishable from the equivalent domains of HLA-A2, the average root mean square (rms) deviation being 0.66 Å.

Examination of the 52 amino acids that differ between the $\alpha_1\alpha_2$ domains of the two class I molecules reveals that the side chains of 13 face into the peptide binding groove (Fig. 1). Seven of these residues in H-2K^b interact with either or both of the bound peptides through hydrogen bonding or van der Waals interactions. Thus, any differences in the shape and chemical nature of the groove must arise from the type and location of these polymorphic residues as the other residues are conserved (Table 1). The shape of the binding groove can be easily visualized through the use of a solvent-accessible surface. Although the shapes of the grooves of H-2K^b bound with either VSV-8 (Fig. 2A) or SEV-9 (Fig. 2B) peptide are similar, the shapes of the H-2K^b and HLA-A2 grooves differ [for HLA-A2, see figure 3b in (6)]. In H-2K^b, an additional deep recess (or indentation) lies mid-floor in the peptide binding groove formed by the β sheet of $\alpha_1\alpha_2$ domains. This deep recess of H-2K^b perfectly accommodates the bulky side chain of Tyr^{P5} of the VSV-8 peptide or Tyr^{P6} of the SEV-9 peptide (Fig. 2C). It should be noted that these tyrosines of VSV-8 and SEV-9 peptides are consensus residues of H-2K^b–restricted peptides and are, therefore, called "anchor" residues (9). The anchor residue has been defined as an invariant residue or a few closely related residues that represent the allele-specific peptide motifs (9). As pointed out, these motifs do not necessarily represent "peptide binding motifs," but rather the possible outcome of peptide processing. Consequently, the anchor residues would not always be responsible for the specific binding to MHC molecules. In contrast to H-2K^b, the corresponding region of the groove of HLA-A2 is much shallower (or mounted) and, therefore, cannot accommodate such a bulky side chain without causing severe steric hindrance. This dramatic transformation of the groove shape in H-2K^b, compared to

HLA-A2, is primarily caused by the replacement of bulky residues with smaller residues, Phe[9] to Val, Arg[97] to Val, and Tyr[99] to Ser, and partially by a conformational change in the Tyr[116] side chain (Fig. 2, A and B). In H-2K^b, the side chain of Tyr[116] faces Val[97], whereas in HLA-A2 the side chain of Tyr[116] is rotated toward Asp[77]. However, it is not clear whether such a conformational change of the Tyr[116] side chain results from the binding of different peptides or from different interactions with the neighboring residue at position 97 (Val in H-2K^b; Arg in HLA-A2).

The deep recess in the middle of the groove makes the H-2K^b molecule distinctive among class I molecules. For example, H-2K^b preferentially binds an octamer peptide, whereas the other known class I molecules bind nonamers (9). The NH_2- and COOH-termini of each peptide are fixed at both ends of the groove through an extensive hydrogen bonding network. Consequently, the conformation of the middle portion of the peptide is most variable and greatly dependent on the size, shape, and nature of the residues lining the central portion of the groove. The deep recess in the groove of H-2K^b molecule appears to account for the binding of a one-residue shorter peptide (octamer). By contrast, other class I molecules such as HLA-A2 that have a shallow groove would force the middle portion of the bound peptide to have a more kinked conformation while still conserving interactions at the NH_2- and COOH-termini of the peptide, as seen for the H-2K^b–SEV-9 complex (Fig. 2C).

Peptide binding pockets. Although various types of recesses, indentations, and ridges are visible on the peptide binding groove (Fig. 2, A and B), finding exact locations of pockets (subsites) for specific side chains of the peptide is somewhat difficult. The term "pocket" is equivalent to the term "subsite" widely used in enzymology (*20*). That is, a pocket of the peptide binding groove is the unit with an individual affinity to the corresponding side chain (or residue) of a peptide. Some pockets have a well-shaped structure (such as a recess or indentation) that is specific for only one side chain, but others do not, and in some instances the boundary between two pockets is ambiguous. Also, a large pocket could accommodate more than one side chain of the peptide.

One way to locate the positions of pockets, perhaps the most direct way, is to

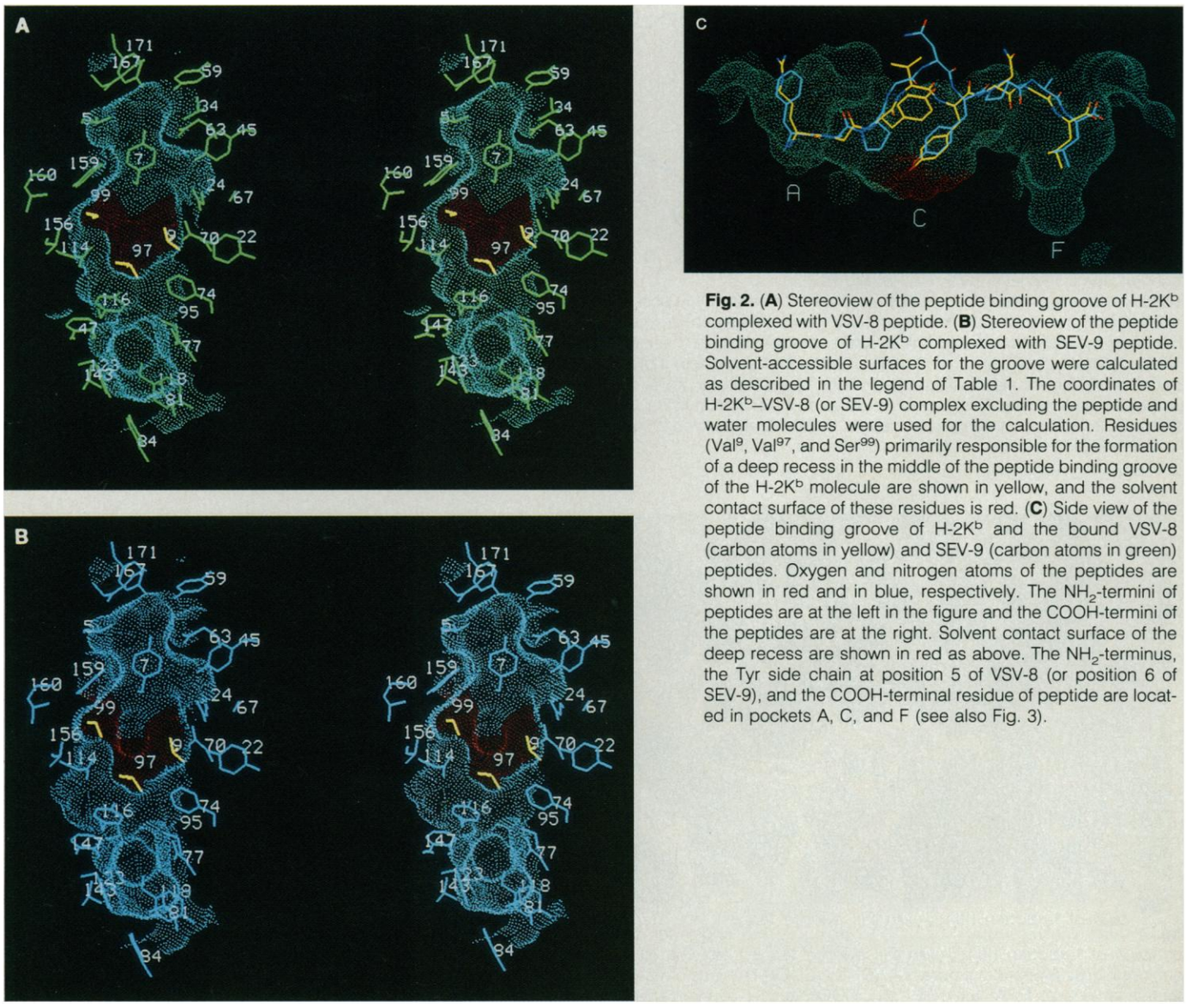

Fig. 2. (**A**) Stereoview of the peptide binding groove of H-2K^b complexed with VSV-8 peptide. (**B**) Stereoview of the peptide binding groove of H-2K^b complexed with SEV-9 peptide. Solvent-accessible surfaces for the groove were calculated as described in the legend of Table 1. The coordinates of H-2K^b–VSV-8 (or SEV-9) complex excluding the peptide and water molecules were used for the calculation. Residues (Val[9], Val[97], and Ser[99]) primarily responsible for the formation of a deep recess in the middle of the peptide binding groove of the H-2K^b molecule are shown in yellow, and the solvent contact surface of these residues is red. (**C**) Side view of the peptide binding groove of H-2K^b and the bound VSV-8 (carbon atoms in yellow) and SEV-9 (carbon atoms in green) peptides. Oxygen and nitrogen atoms of the peptides are shown in red and in blue, respectively. The NH_2-termini of peptides are at the left in the figure and the COOH-termini of the peptides are at the right. Solvent contact surface of the deep recess are shown in red as above. The NH_2-terminus, the Tyr side chain at position 5 of VSV-8 (or position 6 of SEV-9), and the COOH-terminal residue of peptide are located in pockets A, C, and F (see also Fig. 3).

find a recess (or indentation) that accommodates specific side chains (or residues) of the bound peptide. Another way is to calculate the solvent-accessible surfaces with the use of probes of different radii and to find residues that are accessible to a 1.4 Å probe (corresponding to the radius of a water molecule) but not to a larger radius probe, say 3.5 Å, as described (*13*). We systematically calculated surface areas with probes of radii ranging from 1.4 to 5.0 Å. By these methods we not only identified the locations of pockets but also found variations in their depths (Table 1). A deep pocket is one that has residues predominantly accessible to a 1.4 Å probe but not to a probe >3.5 Å. A shallow pocket has residues mainly accessible to a 3.5 Å probe but not to a 5.0 Å probe. Our analysis suggests that so-called pockets A, B, C, and F are deep and that pockets D and E are shallow, according to the nomenclature of Saper *et al.* (*13*). Although the exact location of pocket C is quite different in H-2K^b and HLA-A2 structures, all other pockets have more or less the same locations. However, the sizes of pockets B and, especially, C are significantly different (as shown below). Six buried residues are assigned to pocket C in H-2K^b, but only three residues are assigned to the equivalent pocket in HLA-A2. Thus, pocket C of H-2K^b is not only deeper but also larger than that of HLA-A2.

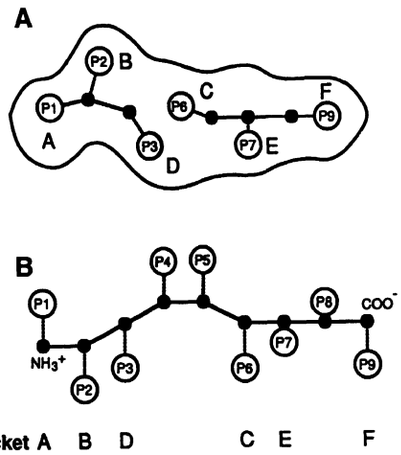

Fig. 3. Peptide interaction with class I molecules. (**A**) Representation of the conformation of SEV-9 peptide and their side chain locations in the groove of H-2K^b molecule. The locations of pockets are shown by A, B, C, D, E, and F in a view similar to that in Fig. 2B. Closed and open circles represent the backbone Cα and the side chains (P1 to P9) of the peptide, respectively. The peptide backbone connections are shown in solid lines, while the side chain connections appear as dotted lines. The side chains at P1, P2, P3, P6, P7, and P9 fit into pockets A, B, D, C, E, and F, respectively. (**B**) Schematic representation of the orientation of side chains of SEV-9 peptide in a view similar to that in Fig. 2C. The side chains at P1, P4, and P5 of the peptide protrude toward the solvent and, hence, can be recognized by the T cell receptor. The side chains at P2, P3, P6, and P9 face into the groove and are accommodated in the corresponding pocket and, hence, not available for T cell recognition. The amino and carboxyl groups of the peptide interact with the residues lining in pockets A and F, respectively. The structures of pockets A and F are well conserved among many class I molecules, but those of pockets B to E differ from one class I molecule to another with respect to size and chemical nature. Also, the P5 side chain, instead of P6, could be accommodated in pocket C in some cases. This diagram is based on the assumption that the optimal length of peptide is a nonamer for a putative class I molecule. When the optimal length of peptide is an octamer, the P6 to P9 peptide residues correspond to those of P5 to P8.

The location of pockets A to F of H-2K^b and the location and orientation of side chains P1 to P9 of peptide bound to H-2K^b are diagrammed in Fig. 3, A and B. Since the backbone conformations of VSV-8 and SEV-9 peptides bound to H-2K^b are very similar, only a nonamer peptide is shown. The side chains of P1, P2, P3, P6 (P5 in VSV-8 peptide), P7 (P6 in VSV-8), and P9 (P8 in VSV-8) fit into pockets A (near residues 7 and 171), B (near 24 and 45), D (near 99 and 156), C (near 9 and 97), E (near 114 and 152), and F (near 77 and 143), respectively. Thus, all the peptide side chains that interact with the corresponding pockets extend toward the pocket either vertically (P6 and P9) or horizontally (P2, P3, and P7), except for the first residue of the peptide (P1), which extends toward the solvent.

Pockets A and F and the orientation of peptide binding. Although many hydrogen bonds are involved between the VSV-8 or SEV-9 peptide and H-2K^b (*11*, table 4), pockets A and F contribute to several hydrogen bonds that are almost identical in the two peptide complexes. Thus, highly conserved residues at pockets A and F of H-2K^b form common hydrogen bonds with these viral peptides (Table 2).

Pocket A accommodates the NH_2-terminus of the peptide, and the precise positioning of the NH_2-terminus is in large part achieved by the three highly conserved tyrosines at positions 7, 159, and 171 (Table 2 and Fig. 4A). The hydroxyl groups of these tyrosines form nearly optimal hydrogen bonds (2.7 to 3.0 Å) with the amino group (N1) and carbonyl oxygen (O1) of

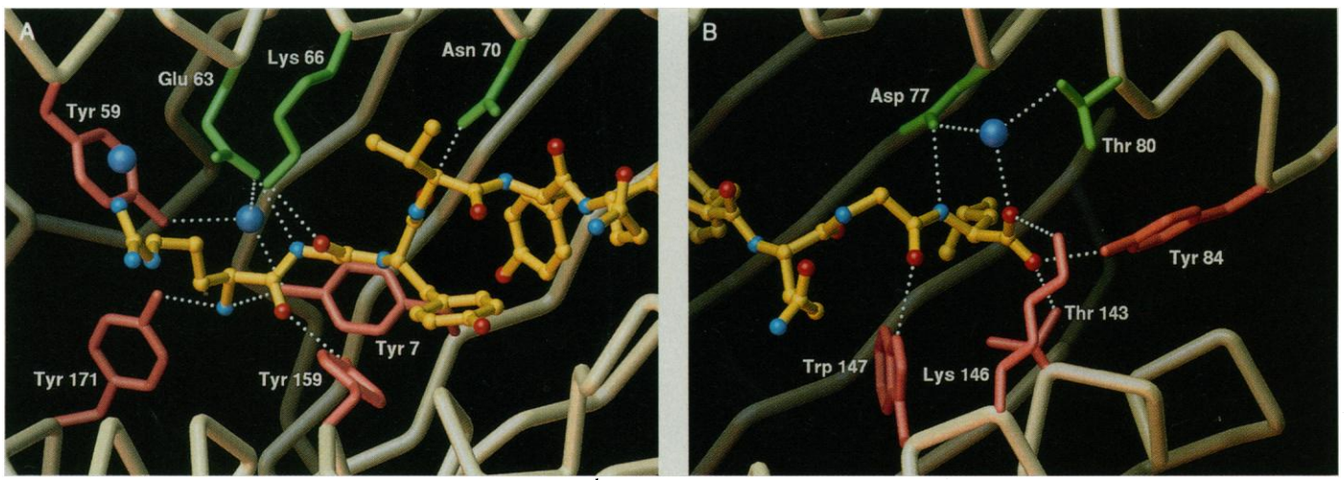

Fig. 4. The highly conserved structures of pockets A and F for the formation of hydrogen bonds with the peptide termini. (**A**) The NH_2-terminus of VSV-8 peptide at pocket A. (**B**) The COOH-terminus of VSV-8 peptide at pocket F. At the NH_2- and COOH-termini of the peptide backbone hydrogen bonds (dotted lines) are formed in pockets A and F, respectively, with highly conserved residues (red) and less conserved residues (green). Conserved water molecules in both VSV-8 and SEV-9 complexes are shown in blue. For details see Table 2.

the first residue of the peptide. In addition, the peptide backbone atoms at P2 and P3 form hydrogen bonds with Glu^{63}, Lys^{66}, and Asn^{70}; although these residues are less conserved, they are sufficiently homologous to form "conserved" hydrogen bonds. Thus, the NH_2-terminal peptide backbone interacts with the bottom of pocket A through an extensive hydrogen bond network. The formation of so many hydrogen bonds in the buried pocket, especially with the conserved tyrosines, must provide significant binding energy. Conversely, the P1 side chain points up toward the solvent so that various amino acids could be accommodated at this position. This may explain why there is no evident preference for the P1 side chain in many class I molecules examined so far (*9, 10*). However, any chemical modification of the α-amino group would destroy several hydrogen bonds made with class I molecules. Also, substitutions in the class I molecule itself would likely destroy the highly conserved electrostatic environment in pocket A. Of particular interest is the nonclassical class I molecule, H-2M3, which specifically binds N-formylated mitochondrial and bacterial peptides and has a Phe at position 171 (*21*). Computer-aided modeling based on the H-2K^b structure showed that the extra space formed by the replacement of Tyrosine with phenylalanine could accommodate an N-formylated NH_2-terminus in this pocket. Although the hydrogen bond between the formylated terminus and the phenylalanine can no longer be formed, the formylated terminus could undergo a hydrogen bonding with the hydroxyl group of Tyr^7.

The COOH-terminus of the peptide is located at the other end of the binding groove in pocket F (Fig. 4B). Although the bottom part of pocket F is hydrophobic in most class I molecules (except in HLA-B27), the entrance to the pocket is hydrophilic. The carboxyl group of the last residue and carbonyl oxygen of the penultimate residue of the peptide make extensive hydrogen bonds, with the highly conserved side chains of Tyr^{84}, Thr^{143}, Lys^{146} (salt bridge), and Trp^{147} and with the moderately conserved side chain of Asp^{77} (Table 2). However, the buried hydrogen bond formed with Thr^{143} would be expected to be stronger than the exposed hydrogen bonds with Tyr^{84} and Trp^{147}. Unlike pocket A, the side chain of the COOH-terminus (Leu^{P8} in VSV-8 and Leu^{P9} in SEV-9) points toward the floor of the binding groove. Thus, the chemical nature and size of pocket F should restrict the amino acid side chains that can be accommodated. Bulky aromatic residues clearly cannot fit in this pocket. However, the pocket depth in H-2K^b suggests that a longer aliphatic moiety would bind tighter to this pocket than leucine does (Fig. 2C). Indeed, in HLA-B27 a longer arginine side chain fills this pocket and presumably forms a buried salt bridge with Asp^{116} (*14*) (as below).

Thus, both the NH_2- and COOH-termini of the peptide specifically interact with the opposite ends of the groove through extensive electrostatic interactions. This suggests that the specific and extensive hydrogen bonding in pockets A and F determine the correct positioning and, thereby, a general orientation of peptide binding to class I molecules. These features are similar to those described for the interpretation of a mixture of peptides bound to HLA-B27 (*14*). Consequently, the role of pockets A and F, which bind the NH_2- and COOH-termini of the peptide, is likely to be universal for all human and murine class I molecules.

Another interesting feature is the "closed" nature of pockets A and F, which restricts the length of the peptide binding groove in class I molecules. By contrast, class II molecules can bind much longer peptides (13 to 17 amino acids); in fact, both ends of a peptide bound to class II molecules have been assumed to protrude from the peptide binding groove (*8*). The closed structure of the pockets at both ends of the class I groove is mainly due to the highly conserved residues Trp^{167} and Tyr^{171} (pocket A) and Tyr^{84} (pocket F), which are replaced with Asp, Pro, and Arg, respectively, in the corresponding class II sequence (*22*). The use of separate α and β chains in class II molecules might also help to open both ends of the groove and allow the binding of longer peptides.

Deep and shallow pockets. Since pockets A and F accommodate the NH_2- and COOH-termini of the peptide, the remaining deep pockets B and C in the middle of the groove appear to determine the sequence specificity of peptide binding in H-2K^b. Indeed, pocket C accommodates the anchor residue Tyr^{P5} of VSV-8 or Tyr^{P6} of SEV-9 (Fig. 2C). In H-2K^b, pocket B does not appear to be important for the selection of peptides, presumably because it is too small to accommodate a large side chain. However, in HLA-A2, pocket B is a

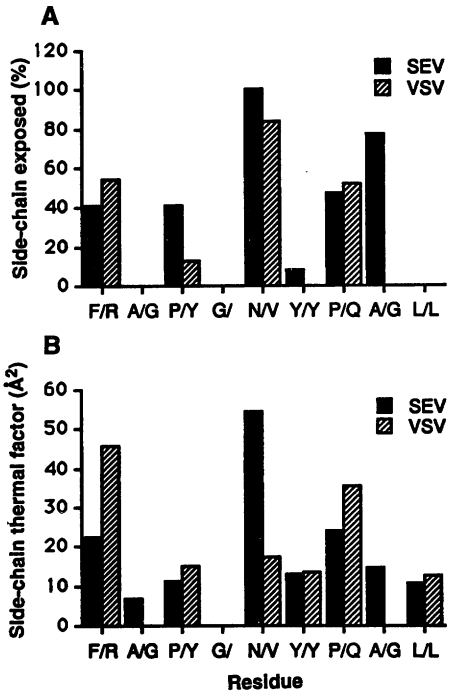

Fig. 5. Fractional solvent-accessible surface (**A**) and thermal factor (**B**) of side chains of VSV-8 and SEV-9 peptides bound to H-2K^b. (A) Solvent-accessible surfaces of the bound peptides were calculated from the coordinates of H-2K^b–VSV-8 and H-2K^b–SEV-9 complexes (excluding the water molecules), as described in the legend of Table 1. Solvent-accessible surfaces of the unbound peptides were calculated from the coordinates of VSV-8 and SEV-9 peptides alone. (B) Side chain thermal factors of the peptides bound to H-2K^b molecules.

Table 2. Hydrogen bonds between peptide and H-2K^b. Conserved residues in human and murine MHC class I molecules are shown in bold. The first numbers in parentheses represent the conserved residues out of the total class I molecules surveyed. The residue Lys^{146} and the carboxylate of the peptide form a salt bridge. Sequence data were taken from (*41*).

H-2K^b		VSV-8			SEV-9			Conserved
Residue	Atom	Residue	Atom	Distance (Å)	Residue	Atom	Distance (Å)	
Y^7	**OH**	**R^{P1}**	**N**	**2.75**	**F^{P1}**	**N**	**2.60**	**Y (21/21)**
Y^{171}	**OH**	**R^{P1}**	**N**	**2.71**	**F^{P1}**	**N**	**2.71**	**Y (19/20)**
Y^{159}	**OH**	**R^{P1}**	**O**	**2.81**	**F^{P1}**	**O**	**2.91**	**Y (21/21)**
E^{63}	Oε1	G^{P2}	N	3.05	A^{P2}	N	2.89	E,Q,N
K^{66}	Nζ	G^{P2}	O	2.79	A^{P2}	O	2.81	K,R,I,N
N^{70}	Nδ2	Y^{P3}	O	3.03	P^{P3}	O	2.98	N,D,Q,H,T
W^{147}	**Nε1**	**G^{P7}**	**O**	**2.99**	**A^{P8}**	**O**	**2.85**	**W (19/21)**
D^{77}	Oδ2	L^{P8}	N	3.05	L^{P9}	N	2.95	D,S,N
Y^{84}	**OH**	**L^{P8}**	**O**	**2.73**	**L^{P9}**	**O**	**2.82**	**Y (20/21)**
T^{143}	**Oγ1**	**L^{P8}**	**O**	**2.82**	**L^{P9}**	**O**	**2.77**	**T (20/21)**
K^{146}	**Nζ**	**L^{P8}**	**OT**	**2.92**	**L^{P9}**	**OT**	**2.79**	**K (20/21)**

single, prominent, deep indentation in the middle side of the groove and probably accommodates the anchor residues at P2 (as discussed). Thus, the pocket depth or capacity to bury the side chain of bound peptide has a direct impact on the peptide-binding energy since such a pocket prevents the access of water molecules and would potentially realize the maximum hydrophobic and hydrogen bonding energy (*23–25*). Conversely, a shallow pocket does not completely shield that side chain from solvent, presumably leading to less binding energy.

This argument is supported by data showing the solvent accessibility of individual peptide side chains (Fig. 5A) and their thermal factors (Fig. 5B). The crystallographic thermal factor for an atom or residue indicates the degree of its thermal motion or disorder in the crystal. For example, residues, such as a Pro, which have less intrinsic rotational and vibrational freedom, tend to have lower thermal factors. Therefore, it is difficult to correlate precisely solvent accessibility and mobility as expressed by thermal factors (*26*). However, residues that fit into deep pockets clearly tend to have lower thermal factors than residues that fit into shallow pockets. The anchor residues Tyr^{P5} (VSV-8) or Tyr^{P5} (SEV-9) that are buried in pocket C (deep) have low temperature factors, whereas the side chains of Glu^{P6} (VSV-8) and even Pro^{P7} (SEV-9) that are partially accommodated in pocket E (shallow) have much higher temperature factors, indicating that these side chains in pocket E are more mobile (Fig. 5). Thus, shallow pockets D and especially E are likely to be less critical for specific peptide binding than the deeper pockets because the former provide less binding energy. Nonetheless, these pockets are important since they may contribute to the capacity to bind peptides with diverse sequences.

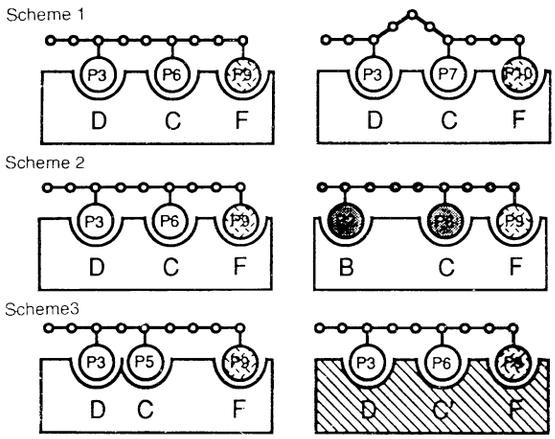

Fig. 6. Pockets in a given class I molecule for selective binding of peptides. The model is based on the assumption that the optimal length of peptide is a nonamer and that the class I molecule has one major pocket (C) and one minor pocket (B or D, or both). It is not clear whether pocket F is responsible for the allele-specific peptide binding. (**Scheme 1**) shows that a class I molecule is capable of binding a slightly longer peptide with the same combination of pockets (in this case, D, C, and F). The optimal length of peptide (a nonamer) binds with the greatest affinity to the class I molecule (left), yet the same class I molecule could bind a slightly longer peptide (in this case, a decamer) by protruding into the middle portion of the peptide (right). (**Scheme 2**) shows that a given class I molecule binds a different set of peptides by using a different set of pockets. This putative class I molecule has one major pocket, C, and the two minor pockets, D (left) and B (right). Thus, this molecule could bind two distinct sets of peptides; both have the common anchor residues at position 6, but only one has a supplemental anchor residue at P3 (in pocket D) and the other at P2 (in pocket B). (**Scheme 3**) shows that the same peptide can bind to different class I molecules. The putative class I molecule on the left has two pockets, D (minor) and C (major), and the other class I molecule on the right also has two pockets, D and C′. Pocket C′ differs from pocket C in that the left molecule accommodates the P5 side chain of peptide, whereas pocket C′ in the right molecule accommodates the P6 side chain of the same peptide. Note that the orientation of the P5 and P6 side chains of the peptide is entirely different when the same peptide binds to the two molecules.

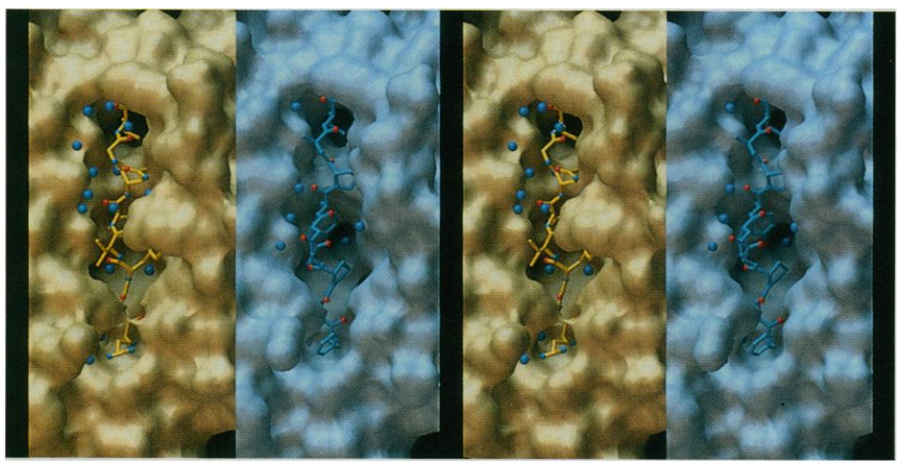

Fig. 7. Double stereoview of the peptide binding groove of H-2K^b complexed with the VSV-8 peptide (left, in yellow) and the SEV-9 peptide (right, in blue). H-2K^b is shown through the use of solvent-accessible surface. Oxygen and nitrogen atoms of the peptides are shown in red and in blue, respectively. Bound water molecules are also displayed in blue. The depth of the groove and the relative inaccessibility of peptide bound to MHC class I molecules are illustrated.

Table 3. Pockets and peptide binding motifs. Only residues important for the transformation of pocket structure and specificity are shown. Since residues Tyr^7, Val^{34}, and Glu^{63} in pocket B and residues Tyr^{118}, Tyr^{123}, Ile^{124}, Thr^{143}, and Trp^{147} in pocket F are all conserved among these class I molecules, they are not included in the table. Ser^{99} for H-2K^b and H-2D^b does not participate in the formation of pocket B and is shown in parentheses. Data on the anchor residues restricted to the corresponding class I molecules are taken from (*9*), except for HLA-B27 (*10*). The putative structures of H-2D^b, H-2K^b, and HLA-B27 were modeled based on either H-2K^b–SEV-9 complex structure (for H-2D^b and H-2K^b) or HLA-A2 structure (for HLA-B27) with the use of HOMOLOGY (Biosym) and subsequent energy minimization with DISCOVER (Biosym).

	Pocket B Residue position					Anchor residue at P2
	9	24	45	67	99	
H-2K^b	V	E	Y	A	(S)	—
H-2D^b	E	S	Y	A	(S)	—
H-2K^d	V	A	F	A	F	Y
HLA-A2	F	A	M	V	Y	L
HLA-B27	H	T	E	C	Y	R

	Pocket C Residue position			Anchor residue at P5 (or P6)
	9	97	99	
H-2K^b	V	V	S	Y, F
H-2D^b	E	Q	S	N
H-2K^d	V	R	F	—
HLA-A2	F	R	Y	—
HLA-B27	H	N	Y	—

	Pocket F Residue position			Anchor residue at P8 (or P9)
	81	95	116	
H-2K^b	L	I	Y	L
H-2D^b	L	L	F	M
H-2K^d	A	F	F	I, L
HLA-A2	L	V	Y	V
HLA-B27	L	L	D	K, R

Deep pockets and peptide specificity. Several lines of evidence suggest that pocket B accommodates P2 side chains in many class I molecules and in some is probably the major pocket. First, in the HLA-B27 crystal structure complexed with heterogeneous self-peptides, the extra electron density of the P2 side chain, presumably arginine, extends into pocket B (*10, 14*). Second, the strict positioning of the NH_2-terminus peptide bound to class I molecules automatically restricts the orientation and location of the P2 side chain. In fact, the conformations of VSV-8 and SEV-9 peptides near the NH_2-terminal region are strikingly similar. Therefore, the P2 side chain of peptide is probably accommodated in pocket B of many class I molecules, when the size and chemical nature of the P2 side chain are compatible with those residues lining pocket B. As in H-2K^b, pockets D and E of HLA-B27 also accommodate the P3 and P7 side chains, respectively (*14*). Thus, the remarkable similarity of pocket location and common interactions with specific peptide side chains between H-2K^b and HLA-B27, as well as the observations made above, suggests that in many class I molecules peptides bind in a similar conformation to those observed in the H-2K^b–peptide complex structures (Fig. 3). Thus, the peptide binding scheme shown in Fig. 3 may be applicable to many class I molecules. This scheme suggests not only where the individual side chains of a given peptide are located but also which side chains, such as P4 and P5, may extend into the solvent. The latter notion is supported by the uninterpreted electron density in HLA-A2, which shows that the middle portion of the bound peptides protrudes from the groove (*13*).

We have further analyzed the structural relationship between the deep pockets (B, C, and F) and their corresponding anchor residues for five different class I molecules (murine H-2K^b, -D^b, and -K^d and human HLA-A2 and -B27) (Table 3). The prime residues that determine the size and chemical nature of pocket B are at positions 9, 24, 45, 67, and 99, and those residues appear to be associated with the respective P2 side chains. For example, H-2K^d molecules predominantly bind peptides with a tyrosine at P2 (*9, 27, 28*). Computer-aided modeling predicts that H-2K^d is likely to have the largest pocket B among these class I molecules and that the very hydrophobic pocket B (composed of Val^9, Ala^{24}, Phe^{45}, Ala^{67}, and Phe^{99}) can accommodate the side chain of Tyr^{P2} after a slight adjustment of the peptide main chain. In contrast, HLA-A2, which has a moderate-sized pocket B, tends to bind peptides with smaller P2 residues, such as leucine (*9, 17, 18*). H-2K^b, which has the smallest pocket, tends to bind much smaller amino acids, such as Gly^{P2} (VSV-8) and Ala^{P2} (SEV-9) (*19*). In HLA-B27, the negatively charged Glu^{45} may be responsible for the selection of positively charged Arg at P2, as previously suggested (*14*). Modeling also suggests that the size of residues at positions 9, 24, and 99 would be most important. The type of residue at position 9, which lies at the boundary between pockets B and C (Fig. 2A), definitively changes the size and shape of pocket B (as well as C). For example, in HLA-A2, Tyr^{99} together with Phe^9 form a wall (or high ridge) between pockets B and C, resulting in the formation of more defined pockets (indentations) at this location.

A similar analysis was applied to pocket C (Table 3). H-2K^b, which has the deepest pocket C among these class I molecules, binds specifically a peptide with Tyr or Phe at P5. However, H-2K^d, HLA-A2, and HLA-B27 have bulkier residues at positions 9, 97, and 99 that result in a shallow pocket C, which no longer binds large side chains at P5 (or P6). In the case of H-2D^b, the anchor residue Asn^{P5} might interact with Glu^9 and Gln^{97} through hydrogen bonds. Again, computer modeling supports this notion. The model also suggests that hydrogen bonds between Asn^{P5} and Glu^9 and Gln^{97} would be buried provided that the conformation of the peptide at P5 is similar to that of the VSV-8 peptide. Such buried hydrogen bonds should have enough strength and provide sufficient energy to determine the binding specificity to H-2D^b.

Pocket F, in most class I molecules, is hydrophobic and large enough to accommodate a medium-sized hydrophobic residue such as Val or Leu (Table 3 and Fig. 2C). One exception is in HLA-B27, which preferentially binds peptides with a positively charged Arg or Lys as the COOH-terminal residue (*10*). This distinctive feature of HLA-B27 is reflective of the presence of a negatively charged residue Asp^{116} at the base of the pocket (*14*). Although hydrophobic residues at the COOH-terminus of peptides are assigned as the anchor residues in many class I molecules, the residues that pocket F accommodates vary and are not restricted as stringently as other anchor residues in the middle of the peptide sequences (*9, 17, 18*). In 11 H-2K^d–restricted peptides, one of the two assigned anchor residues, Ile^{P9} and Leu^{P9}, occurs in six of the peptides, the remainder being Val, Ala, and Thr, whereas the other Tyr^{P2} occurs in all 11 peptides (*9*). In addition, such a bias toward hydrophobic residues at the COOH-terminus might be due to in vivo peptide processing (*9, 29*). No dominant residues were observed at the COOH-terminus of peptides eluted from purified, empty H-2K^b mixed with randomly synthesized octapeptides in vitro (*19*). Taken together, these data indicate that pocket F lacks the strict selectivity for peptide side chains and that pocket F is functionally a minor pocket despite its depth. This might also be influenced by the near-surface position of the COOH-terminal region of peptide compared to the buried position of the NH_2-terminal region.

Regardless of whether pocket F is major or minor, a close relation exists between the structure of major pockets and the identified anchor residues of their peptide. The structural and physicochemical complementarities between these pockets and peptide side chains must be the molecular basis of peptide binding specificity for MHC class I molecules. This analysis suggests that the limited number of major pockets (probably only one for a given class I molecule) mainly determines the allele-specific peptide binding motif.

A general model for peptide binding. The comparison of conformations between VSV-8 and SEV-9 peptides offers some insight on how a longer peptide could bind to a class I molecule (Fig. 6, scheme 1). As shown, the middle portion of a slightly longer peptide could protrude without much loss of affinity. In fact, the dissociation constants of VSV-8 and SEV-9 peptides are almost identical (about 4 nM) (*19*). The Gly and Pro residues in the middle portion of peptide may allow the peptide to adopt a more kinked conformation, as for the SEV-9 peptide (Gly^{P3} and Pro^{P4}) seen in Fig. 2C.

Although pocket B appears to be the major pocket in many class I molecules, the pocket in H-2K^b does not participate in the binding of either VSV-8 (Gly at P2) or SEV-9 (Ala at P2) peptides. However, H-2K^b may actually use the pocket to bind a distinct set (or sets) of peptide sequences such as the OVA-8 peptide (ovalbumin 257–264, SIINFEKL) (*30*), which contains a larger residue at P2. In the H-2K^b–SEV-9 complex, the Cβ of Ala^{P2} points toward pocket B, an indication that the side chain of Ile^{P2} could be accommodated partly in pocket B and partly in pocket C. Thus, pocket B may also participate in the selective binding of OVA-like peptides in H-2K^b. Although pocket B in H-2K^b is minor, the combined usage of major and minor pockets would allow the same class I molecule to bind a distinct set of peptides (Fig. 6, scheme 2). In H-2K^b the VSV-8 and SEV-9 peptides interact with pocket D (minor) and pocket C (major), whereas the OVA peptide probably interacts with pocket B (minor) and pocket C (major). Here, pocket C is common to both cases and, therefore, determines the H-2K^b–specific peptide motif. In contrast, pockets B (for OVA-8) and D (for VSV-8 and SEV-9) must be supplemental for peptide binding. Thus, it appears that class I molecules do

not fully use all six pockets for peptide binding; rather they preferentially favor one major pocket and one or two minor pockets in the selection of peptides. Such a limited usage of pockets would allow binding of a myriad of different peptides and would account for the broad specificity of peptide binding to MHC class I molecules.

An alternative feature of class I–peptide interactions is illustrated in scheme 3. The same peptide could bind to different class I molecules. For example, the OVA-9 peptide (ESIINFEKL) binds to both H-2D^b and H-2K^b (*31*). In this case, Ile^{P3} and Asn^{P5} of OVA-9 peptide may interact with pockets D and C of H-2D^b, while Ile^{P3} and Phe^{P6} of the same peptide may interact with pocket D and C′ of H-2K^b. The anchor residue for H-2D^b is Asn^{P5}, and that for H-2K^b is Phe^{P6}. However, the conformation of OVA-9 bound to H-2D^b must be quite different from that of OVA-9 bound to H-2K^b because the P5 side chain that faces inward to the groove of H-2D^b would face outward to the solvent when the same peptide binds to H-2K^b. This conformational change in a peptide bound to different class I molecules would be of particular importance when one considers the interactions between a class I–peptide complex and a T cell receptor.

Inferences for peptide recognition. The distinctive characteristic of class I–peptide interactions is promiscuity compared with other protein-ligand interactions, most of which are highly specific. Let us consider how a class I molecule can bind so many different peptides. As described earlier (*11*), a large number of hydrogen bonds (21 to 36), van der Waals interactions (88 to 119 contacts), and hydrophobic interactions (604 to 681 Å^2 of buried surface of peptide) are involved in peptide binding. This number of interactions is closer to that in protein-protein rather than in protein-ligand interactions (*32–35*). Most of the interactions between the class I molecule and the peptide are somewhat nonspecific. Almost all of the hydrogen bonds are formed with the peptide backbone. The large number of van der Waals contacts is due to the deep burial of the bound peptide within the groove of class I molecules (Fig. 7). These unusual features promote promiscuous rather than specific interactions while still maintaining high affinity.

The class I molecule can select an allele-specific peptide partly because of structural complementarity between the allele-specific pocket and anchor residue and partly because of the stabilization of class I structure by a bound peptide. As discussed above, the specificity derived from structural complementarity seems to be achieved by only a single major pocket and a single anchor residue. Indeed, it has been reported that in class II molecules only a single peptide side chain is crucial to binding, and most of the side chains are not required for high affinity binding (*36*). Similarly, a single amino acid substitution of a peptide anchor residue in H-2K^b decreases the binding affinity only by a factor of 10 (*37*). Importantly, this small decrease in affinity has the profound biological effect of increasing the dissociation rate of the bound peptide enough to prevent adequate time for presentation to T cells at the cell surface, because class I molecules devoid of peptides are very unstable (*38, 39*). Consequently, only peptides with an allele-specific anchor residue may provide sufficient stability to class I molecules to ensure transport and presentation of such peptides for T cell recognition.

REFERENCES AND NOTES

1. A. Townsend and H. Bodmer, *Annu. Rev. Immunol.* **7**, 601 (1989).
2. P. Kourilsky and J.-M. Claverie, *Adv. Immunol.* **45**, 107 (1989).
3. P. J. Bjorkman and P. Parham, *Annu. Rev. Biochem.* **59**, 253 (1990).
4. T. J. Tsomides and H. Eisen, *J. Biol. Chem.* **266**, 3357 (1991).
5. P. J. Bjorkman *et al.*, *Nature* **329**, 512 (1987).
6. T. P. J. Garrett, M. A. Saper, P. J. Bjorkman, J. L. Strominger, D. C. Wiley, *ibid.* **342**, 692 (1989).
7. G. M. Van Bleek and S. G. Nathenson, *ibid.* **348**, 213 (1990).
8. A. Y. Rudensky, P. Preston-Hurlburt, S.-C. Hong, A. Barlow, C. A. Janeway, Jr., *ibid.* **353**, 622 (1991).
9. K. Falk, O. Rötzschke, S. Stevanovic, G. Jung, H.-G. Rammensee, *ibid.* **351**, 290 (1991).
10. T. S. Jardetzky, W. S. Lane, R. A. Robinson, D. R. Madden, D. C. Wiley, *ibid.* **353**, 326 (1991).
11. D. H. Fremont, M. Matsumura, E. A. Stura, P. A. Peterson, I. A. Wilson, *Science* **257**, xxx (1992).
12. P. J. Bjorkman *et al.*, *Nature* **329**, 506 (1987).
13. M. A. Saper, P. J. Bjorkman, D. C. Wiley, *J. Mol. Biol.* **219**, 277 (1991); *Cell*, in press.
14. D. R. Madden, J. C. Gorga, J. L. Strominger, D. C. Wiley, *Nature* **353**, 321 (1991).
15. Abbreviations for the amino acid residues are: A, Ala; C, Cys; D, Asp; E, Glu; F, Phe; G, Gly; H, His; I, Ile; K, Lys; L, Leu; M, Met; N, Asn; P, Pro; Q, Gln; R, Arg; S, Ser; T, Thr; V, Val; W, Trp; and Y, Tyr.
16. T. N. M. Schumacher *et al.*, *Nature* **350**, 703 (1991); W. M. Kast *et al.*, *Proc. Natl. Acad. Sci. U.S.A.* **88**, 2283 (1991).
17. D. F. Hunt *et al.*, *Science* **255**, 1261 (1992).
18. R. A. Henderson *et al.*, *ibid.*, p. 1264.
19. M. Matsumura, Y. Saito, M. R. Jackson, E. S. Song, P. A. Peterson, *J. Biol. Chem.*, in press.
20. A. Fersht, *Enzyme Structure and Mechanism* (Freeman, New York, 1985).
21. C.-R. Wang, B. E. Loveland, K. F. Lindahl, *Cell* **66**, 335 (1991).
22. J. H. Brown *et al.*, *Nature* **332**, 845 (1988).
23. M. Matsumura, W. J. Becktel, B. W. Matthews, *ibid.* **334**, 406 (1988).
24. M. Karpusas, W. A. Baase, M. Matsumura, B. W. Matthews, *Proc. Natl. Acad. Sci. U.S.A.* **86**, 8237 (1989).
25. A. E. Eriksson *et al.*, *Science* **255**, 178 (1992).
26. T. Alber, S. Dao-pin, J. A. Nye, D. C. Muchmore, B. W. Matthews, *Biochemistry* **26**, 3754 (1987).
27. O. Rötzschke *et al.*, *Nature* **348**, 252 (1990).
28. K. Falk *et al.*, *J. Exp. Med.* **174**, 425 (1991).
29. K. Falk, O. Rötzschke, H.-G. Rammensee, *Nature* **348**, 248 (1990).
30. F. R. Carbone and M. J. Bevan, *J. Exp. Med.* **169**, 603 (1989).
31. P. Langlade and P. A. Peterson, unpublished data.
32. J. Janin and C. Chothia, *J. Biol. Chem.* **256**, 16027 (1990).
33. D. R. Davies, E. A. Padlan, S. Sheriff, *Annu. Rev. Biochem.* **59**, 439 (1990).
34. R. L. Stanfield, T. M. Fieser, R. A. Lerner, I. A. Wilson, *Science* **248**, 712 (1990).
35. J. M. Rini, U. Schulze-Gahmen, I. A. Wilson, *ibid.* **255**, 959 (1992).
36. T. S. Jardetzky *et al.*, *EMBO J.* **9**, 1797 (1990).
37. Y. Saito, M. Matsumura, P. A. Peterson, unpublished work.
38. H.-G. Ljunggren *et al.*, *Nature* **346**, 476 (1990).
39. T. N. M. Schumacher *et al.*, *Cell* **62**, 563 (1990).
40. M. L. Connolly, *J. Appl. Crystallogr.* **16**, 548 (1983).
41. J. Klein, *Natural History of the Major Histocompatibility Complex* (Wiley, New York, 1986), center page diagram.
42. M. Carson, *J. Mol. Graph.* **5**, 103 (1987).

43. We thank M. E. Pique for the preparation of Figs. 4 and 7; Y. Saito and E. A. Stura for their earlier invaluable contributions on H-2K^b protein purification and crystallization, respectively; and J. Arevalo, U. Schulze-Gahmen, and R. L. Stanfield for help with computation. Supported in part by NIH grant CA-97489 (P.A.P.) and training grant CA-09523 (D.H.F.). This is publication 7468-MB from The Scripps Research Institute.

26 June 1992; accepted 22 July 1992